Using FoxP2 to Distinguish Direct and Indirect Basal Ganglia Pathways for Vocal Learning in Songbirds

Aditi Jagannathan[1,2], Mira Nigudkar[1,3], Sarah W Bottjer[1]

[1]Section of Neurobiology, University of Southern California, Los Angeles, CA 90089 USA
[2]Current affiliation: Netherlands Institute for Neuroscience, Amsterdam, The Netherlands
[3]Current affiliation: Loyola University Chicago, Stritch School of Medicine, USA

Correspondence to: Sarah W. Bottjer, Section of Neurobiology, University of Southern California, 3641 Watt Way, Los Angeles, CA 90089 (bottjer@usc.edu)

Ethics approval statement

This study was approved by the Animal Care and Use Committee at the University of Southern California and is therefore in compliance with the US National Research Council's "Guide for the Care and Use of Laboratory Animals," and the US Public Health Service's "Policy on Humane Care and Use of Laboratory Animals".

Acknowledgements

This research was supported by NSF grant 1940957. We thank Dr. Jason Junge and Dr. Arkadi Shwartz of the Translational Imaging Center at the USC Michelson Center for Convergent Bioscience for their assistance in training. We thank Dr. Hugh C. Hemmings for the gift of antibody to DARPP-32.

Conflicts of Interest

The authors declare no conflict of interest.

ABSTRACT

Vocal learning in songbirds provides a powerful experimental model for motor skill learning. The cortico-basal ganglia pathways that mediate vocal learning in zebra finches (*Taeniopygia guttata*) are localized in two parallel circuits. These circuits traverse a cortical region (LMAN), a specialized region of the basal ganglia essential for vocal learning (Area X), and a region of dorsomedial thalamus (DLM). Area X, which contains both striatal and pallidal neurons, includes functional analogs of mammalian direct and indirect pathways that may have opposing effects and thereby increase or inhibit thalamic activity respectively. Direct pallidal neurons of Area X send inhibitory projections to DLM, whereas indirect pallidal neurons form intrinsic connections onto DLM-projecting neurons. We used tract-tracing techniques to label direct pallidal Area X→DLM projection neurons and immunohistochemical techniques to label neurons expressing the transcription factor FoxP2 in adult and juvenile male zebra finches. Our results showed that DLM-projecting neurons in Area X did not express FoxP2 in either adults or juveniles. We also observed a population of large neurons that expressed FoxP2 but were not retrogradely-labeled from DLM. A marker of striatal neurons (DARPP-32) did not co-localize with FoxP2 in most of these large neurons, providing evidence that they may form a class of putative indirect pallidal neurons. Our findings offer FoxP2 as a possible marker for indirect pallidal neurons and support the existence of different subpopulations of neurons that likely correspond to direct and indirect pathways within Area X.

1. INTRODUCTION

During motor skill learning, cortico-basal ganglia circuits compare feedback of self-generated motor output to a memorized goal behavior. Similar to humans, zebra finches (*Taeniopygia guttata*) learn vocal sounds from adult tutors during a restricted window of development (Bottjer & Arnold, 1986; Doupe & Kuhl, 1999). Cortico-basal ganglia circuits mediate evaluations of similarity between self-generated utterances and memorized tutor sounds, allowing juvenile birds to refine their babbling to match the goal (tutor song).

The basal ganglia in songbirds includes a specialized region essential for vocal learning and behavior called Area X which receives input from two sensorimotor cortical regions that also regulate song-related functions: HVC and LMAN (Bottjer, Halsema, Brown, & Miesner, 1989; Nixdorf-Bergweiler, Lips, & Heinemann, 1995; Nottebohm, Stokes, & Leonard, 1976; Sanchez-Valpuesta et al., 2019; Scharff & Nottebohm, 1991; Sohrabji, Nordeen, & Nordeen, 1990; Vates & Nottebohm, 1995). Area X sends inhibitory projections to a dorsal thalamic nucleus (DLM), which projects back to LMAN to form a feedback loop (Luo, Ding, & Perkel, 2001; Luo & Perkel, 1999b; Nixdorf-Bergweiler et al., 1995; Vates & Nottebohm, 1995). Previous work showed that the Area X→DLM→LMAN pathway consists of CORE and SHELL subregions, forming two parallel topographically organized circuits (Fig. 1a) (Bottjer et al., 1989; Gale, Person, & Perkel, 2008; Iyengar, Viswanathan, & Bottjer, 1999; Johnson & Bottjer, 1992; Johnson, Sablan, & Bottjer, 1995; Luo et al., 2001; Person, Gale, Farries, & Perkel, 2008). Both CORE and SHELL loops are essential for learning (Achiro & Bottjer, 2013; Achiro, Shen, & Bottjer, 2017; Bottjer & Altenau, 2010), but precise structure-function relationships have been difficult to establish.

The output of the CORE pathway from LMAN drives vocal production in juvenile birds through its projection to motor cortex (RA) (Aronov, Andalman, & Fee, 2008; Bottjer, Miesner, & Arnold, 1984; Scharff & Nottebohm, 1991). In contrast, the output of LMAN-SHELL projects to a region of motor cortex (AId) adjacent to RA that lacks direct motor targets, but instead forms a transcortical loop that converges with information from Area X in DLM (Fig. 1a) (Bottjer, Brady, & Cribbs, 2000). Lesions of AId disrupt accurate imitation of the tutor song but do not impact vocal motor output in juvenile songbirds (Bottjer & Altenau, 2010). This pattern of findings indicates that SHELL circuitry does not drive vocal motor output, but may play an associative-limbic role in evaluating vocal output. The organization of these CORE and SHELL loops is highly similar to the sensorimotor and associative-limbic circuits of mammalian basal ganglia (Graybiel, 2008; Redgrave et al., 2010; Yin & Knowlton, 2006).

Analogs of mammalian direct and indirect pathways of the basal ganglia have been found within Area X of songbirds. Area X contains striatal medium spiny neurons (MSNs), interneurons, and pallidal neurons. In the direct (DIR) pathway, MSNs make inhibitory connections onto pallidal cells, which form calyceal inhibitory synapses on neurons in DLM (Fig. 1b) (Carrillo & Doupe, 2004; Gale et al., 2008; Luo & Perkel, 1999a, 1999b; Person et al., 2008; Reiner, Laverghetta, Meade, Cuthbertson, & Bottjer, 2004). However, Farries, Ding, and Perkel (2005) reported a population of local pallidal neurons in Area X that do not project to DLM, but instead make axonal contacts with DIR DLM-projecting neurons. These large non-projecting neurons express the GABA synthetic enzyme glutamic acid decarboxylase (GAD) (Luo and Perkel (1999b). In addition, DLM-projecting neurons are surrounded by baskets of inhibitory GAD+ processes (Luo & Perkel, 1999b). This pattern is consistent with the idea that the non-projecting population represents indirect (IND) pallidal neurons that form intrinsic inhibitory projections onto DIR neurons of Area X (Fig. 1b). In addition, DIR and IND classes of pallidal neurons in Area X are distinguished by their patterns of firing, which correspond to GPi-like and GPe-like neurons in primates (Goldberg, Adler, Bergman, & Fee, 2010). Because DIR and IND pathways in songbirds cannot be reliably identified by the expression of D1 versus D2 receptors in striatal spiny neurons, their patterns of connectivity remain relatively unknown (Kubikova, Wada, & Jarvis, 2010; Xiao et al., 2021). The goal of our study was to distinguish between these direct and indirect neurons, paving the way to investigate how these pathways play distinct roles in vocal learning.

The transcription factor FoxP2 may serve as one possible marker of indirect non-projecting pallidal neurons in Area X. FoxP2 is essential for human vocal development, with mutations leading to speech disorders such as childhood apraxia (den Hoed & Fisher, 2020). Likewise, disruptions of the FoxP2 gene or overexpression of an miRNA that downregulates FoxP2 in Area X of juvenile songbirds cause vocal deficits and incomplete vocal learning in songbirds (Haesler et al., 2007; Shi et al., 2018). Single nucleus RNA sequencing showed that a cluster of cells in Area X identified as pallidal formed two subgroups: one expressed the gene for enkephalin (ENK) and the other expressed the gene for FoxP2 (Xiao et al., 2021). Because ENK is expressed in DLM-projecting pallidal neurons in songbirds (Carrillo & Doupe, 2004), this pattern suggested that the direct neurons that send a projection to DLM would not express FoxP2, while the indirect non-projecting pallidal neurons would be FoxP2+ (Fig. 1b). To test this idea, we used tract-tracing techniques to label direct pallidal Area X→DLM projection neurons and immunohistochemical techniques to label neurons expressing FoxP2.

Distinguishing between the direct and indirect neurons in Area X will facilitate the investigation of functional differences between direct and indirect pathways during vocal motor development.

2. MATERIALS AND METHODS

2.1 Subjects

All animal procedures were performed in accordance with national regulatory guidelines and followed protocols approved by the Animal Care and Use Committee at the University of Southern California. All birds were bred in group aviaries in our colony and remained with their parents until at least 43-47 days post-hatch (dph), which is beyond the age of adequate tutor song exposure and social experience (Böhner, 1983, 1990; Catchpole & Slater, 1995; Clayton, 1987; Eales, 1985; Immelmann, 1969; Mann & Slater, 1995; Roper & Zann, 2006). Birds were moved to adult sex-specific holding cages in the colony after 90 dph. Surgeries involving intracranial injections of a fluorescent tracer were performed on adult male birds >90 dph (age range: 91-182, n = 4) and juvenile male birds 45 ± 2 dph (n = 3). Following surgery, birds were placed in individual holding cages located in the main colony for three days before being perfused (see below).

2.2 Alexa Fluor 488 Injections

Birds were anesthetized with 1.5-1.7% isoflurane (inhalation) and placed in a stereotaxic apparatus. Stereotaxic coordinates were used to target the location of the thalamic nucleus DLM (dorsolateral nucleus of the medial thalamus; Fig. 1). The head angle was set as follows: we measured the depth of the skull at the bifurcation of the mid-sagittal sinus and at the midline 5 mm anterior to the bifurcation; the head angle was adjusted so that the difference in depth between these two locations was 2.2 ± 0.1. DLM injection coordinates were approximately 0.6 to 0.8 mm anterior and 0.9 to 1.1 mm lateral to the bifurcation of the mid-sagittal sinus at a depth of 4.5 mm. Birds received unilateral left iontophoretic injections of dextran labeled with Alexa Fluor 488 (MW 10,000, 10% in sterile-filtered PBS, ThermoFisher #D-22910) into DLM by applying pulses of current through a silver wire (3-5 µA, 6 sec on/6 sec off) for 20 minutes through a glass pipette (20-30 µm outer diameter). Injections sometimes extended beyond the borders of DLM, but we analyzed retrograde label only within Area X-CORE and SHELL regions. Birds were anesthetized with an injection of 0.04 - 0.06 mL 5% Euthasol 72 hours following surgery and perfused trans-cardially with 0.7% saline followed by 4% periodate-lysine-paraformaldehyde (PLP) fixative (4% para in 0.1 M PB with 0.01 M sodium periodate and 0.1 M

L-lysine; pH 7.8). Brains were removed and post-fixed in 4% paraformaldehyde overnight before being cryo-protected in 25% buffered sucrose solution with 0.005% sodium azide. Brains were frozen sectioned at a thickness of 40 µm in the coronal plane; sections were serially collected in PBS into separate series as described below.

2.3 Immunohistochemistry

2.3.1 Double Label

Sections from four adult birds were stained for FoxP2 and labeled with retrograde Alexa Fluor 488 dye from DLM. Three separate series were processed as follows: Series 1 was stained using rabbit polyclonal anti-FoxP2 (Abcam Cat#ab16046, RRID:AB_2107107), Series 2 was stained using goat polyclonal anti-FoxP2 (Abcam Cat#ab1307, RRID:AB_1268914), and Series 3 was counterstained with thionin for Nissl and coverslipped with Permount (Fisher Scientific). The ab1307 antibody was raised against a synthetic peptide corresponding to amino acids 703-715 (C-terminal) of human FoxP2 (specificity has been described previously, Thompson et al., 2013). The ab16046 antibody was generated using a synthetic peptide corresponding to human FoxP2 aa 700 to the C-terminus conjugated to keyhole limpet haemocyanin (specificity has been described previously, Campbell, Reep, Stoll, Ophir, & Phelps, 2009).

Sections were stained using standard immunohistochemistry techniques. Following three washes in 0.02 M PBS, Series 1 and 2 were blocked in 5% Normal Goat Serum or 5% Normal Rabbit Serum, respectively, for 30-40 minutes and then incubated in the primary antibody (1:1,000) overnight at room temperature. Sections were again triple-washed with PBS and incubated in the appropriate secondary antibody (anti-rabbit-Alexa 594, 1:200, ThermoFisher, #A-11012, made in goat for Series 1; anti-goat-Alexa 594, 1:200, ThermoFisher, #A-11080, made in rabbit for Series 2) for 1 hour. Sections of both series were given three final washes in PBS with the last wash containing 1 µL DAPI (1:10,000, gift from Dr. Jason Junge) before being mounted onto gelatin-coated glass slides. Sections were allowed to air dry before being coverslipped with Prolong Diamond Antifade (ThermoFisher, #P36970).

2.3.2 Triple Label

DARPP-32 is a phosphoprotein that is expressed in virtually all medium spiny neurons of mammals (Ouimet, Langley-Gullion, & Greengard, 1998), although it has been reported to be immunohistochemically detectable in only 30-60% of spiny neurons in birds (Reiner et al., 2004; Reiner, Perera, Paullus, & Medina, 1998; Singh & Iyengar, 2019). In order to test the identity of

cells labeled by FoxP2, we performed triple labeling for FoxP2, DARPP-32, and the retrograde label from DLM in three juvenile birds. During prior analysis of double-labeled tissue, we observed that the anti-FoxP2 used in Series 1 (ab16046) resulted in a higher density of labeled cells compared to the anti-FoxP2 used in Series 2 (ab1307). We therefore created a cocktail of rabbit polyclonal anti-FoxP2 (ab16046, 1:1,000) and mouse monoclonal anti-DARPP-32 (1:30,000, C24-6a, gift from Dr. Hugh C. Hemmings, specificity validated in Hemmings and Greengard (1986) and see Durstewitz, Kroner, Hemmings, and Gunturkun (1998) for pigeon data); alternate sections were stained for Nissl. The same blocking and primary staining procedures outlined for Series 1 above were followed before incubating sections in a secondary antibody cocktail containing anti-rabbit Alexa 594 (1:200, ThermoFisher, #A11012, made in goat) and anti-mouse Alexa 647 (1:200, ThermoFisher, #A-21235, made in goat). All markers used in this study are outlined in Table 1.

2.4 Data Analysis

2.4.1 Overlap Analysis of FoxP2 and Retrogradely-Labeled Neurons in Area X

Patterns of fluorescent label were analyzed in all adult (n = 4) and juvenile (n = 3) birds. Images of Medial Striatum, which includes Area X, were taken with a 40x objective using ZEN imaging software on a confocal microscope (Zeiss LSM 780 inverted microscope or Zeiss 880 LSM inverted microscope) at the USC Translational Imaging Center. The excitation and emission wavelength settings used to image each marker are recorded in Table 1. In order to include all of Medial Striatum, the tilescan feature was used to acquire multiple individual image fields (“tiles”) at different XY positions and stitch them together into one large image. To collect depth information, the ZEN Z-stack feature was used to compile images at various Z positions (“Z-steps”) at the same XY position. Each tissue section consisted of 8-12 Z-steps that were taken approximately 3-4 µm apart. Z-steps were reconstructed into a 3D projection of the section using Imaris image analysis software (Oxford Instruments). 3D projections of individual or multiple fluorescent channels were used in all figures except Figure 6 (insets only) and Figure 7, which were taken at a single Z-step (see below, 2.4.4).

3D projections were analyzed for overlap between neurons retrogradely-labeled from DLM and neurons expressing FoxP2. Retrogradely-labeled cells were classified as being within either Area X-CORE (outlined by DAPI staining), Area X-SHELL (defined conservatively as 500 µm extending from the medial, ventromedial, and ventrolateral edges of Area X-CORE), or “Border” if the boundary between Area X-CORE and SHELL was not easily identifiable by DAPI staining (Iyengar et al., 1999). Each retrogradely-labeled cell was visually inspected at every Z-

step for signs of double-label with FoxP2. Differences in the proportion of retrogradely-labeled neurons that did not express FoxP2 versus retrogradely-labeled neurons that did express FoxP2 were analyzed with a binomial test.

2.4.2 Size Analysis of Retrogradely-Labeled Neurons in Area X

Size analysis of retrogradely-labeled neurons in Area X was performed on four adult birds (n = 100 neurons chosen randomly for analysis out of a total of 469 retrogradely-labeled neurons) and three juvenile birds (n = 87 neurons); see Table 2 below.

Using the Surfaces auto-detection feature in Imaris, 3D models of labeled cells were created based on the 3D projections of individual channels. This allowed us to measure quantitative characteristics of retrogradely-labeled neurons. Cells were detected using automatic absolute intensity thresholding on the Alexa Fluor 488 channel and smoothed with a surface detail of 0.50 µm to ensure close fitting to the staining. Once surfaces were created for labeled cells, we manually inspected each neuron and adjusted the surface to include only the cell body of the neurons, excluding the primary dendrites.

The diameter of neurons retrogradely-labeled from DLM was determined by using the average of two measures of Imaris surfaces: the longest diameter of each cell (referred to as Object-Oriented Bounding Box Length C) and the perpendicular diameter (Object-Oriented Bounding Box Length B); we refer to this measure as the average diameter. This measure is consistent with previous studies in songbirds that reported the average of the major and minor axis of the cell as the diameter (Luo & Perkel, 1999b; Reiner et al., 2004). The average diameter values of each Alexa 488-labeled surface were exported to Microsoft Excel for further analysis. Differences in the size distributions of DLM-projecting neurons between adult and juvenile data were tested with two-sample Kolmogorov–Smirnov (K-S) nonparametric tests.

2.4.3 Size Analysis of FoxP2-Positive Nuclei

Size analysis of FoxP2+ nuclei in Area X-CORE and Area X-SHELL was performed on three adult and two juvenile birds used for overlap analysis. Because the full depth profile of smaller FoxP2+ neurons was not represented in the Z-stack intervals used in the overlap analysis of DIR pallidal cells above, four to five tissue sections per bird were reimaged with smaller Z-stack intervals (0.46 - 0.47 µm apart). This interval ensured that smaller cell types in Medial Striatum, such as medium spiny neurons, were included in the analysis. The boundaries of Area X-CORE in each section were determined using DAPI staining and divided into 212.55 µm x 212.55 µm fields. Images of two randomly selected fields per section were taken at a

magnification of 40x with the updated Z-stack intervals. Two 212.55 µm x 212.55 µm fields per section were also taken for Area X-SHELL: one image was taken ventromedial and the other ventrolateral to the boundaries of Area X-CORE.

The size of FoxP2+ nuclei was determined using the Surfaces feature on the Alexa Fluor 594 channel; surfaces were smoothed with a surface detail of 0.50 µm (Fig. 2). Adjoining surfaces were split based on morphology with a seed point diameter of 3.20 µm to account for the smallest possible striatal medium spiny neuron diameter (Carrillo & Doupe, 2004). Cells were then filtered based on area (>25 μm^2) and distance from the XYZ border (>0.5 µm) to remove cells that were only partially included in the section. Each surface was visually inspected to see if the 3D model matched the FoxP2 staining; if the model's outline was not accurate, the surface was deleted. Additionally, all neurons that exhibited a fusiform appearance were excluded from analysis; these cells are likely putative migratory young neurons (Alvarez-Buylla & Nottebohm, 1988). Measurements of average diameter were calculated as explained in section 2.4.2 and exported to Microsoft Excel for further analysis. Size differences in the diameters of FoxP2+ neurons between adult and juvenile data were tested with a two-sample Kolmogorov–Smirnov (K-S) nonparametric test.

2.4.4 Overlap Analysis of Large FoxP2+ Neurons with DARPP-32

As detailed below in Results, we observed a population of large FoxP2+ neurons that were not retrogradely-labeled from DLM, representing putative IND pallidal neurons. However, because FoxP2 was expressed in nuclei of different sizes along a continuous distribution (see below, Fig. 5), it was not obvious how to segregate non-projecting FoxP2+ pallidal neurons from other FoxP2+ cells. We decided to use nuclear diameter to segregate the putative IND neurons given that their nuclear diameter should be similar to that of DIR DLM-projecting neurons. Based on this idea, we first measured the nuclear diameter of 50 FoxP2- retrogradely-labeled DIR neurons from one adult bird in which DAPI staining was particularly good (Fig. 7). The full depth profile of each DIR neuron was inspected to select the Z-step which included the largest visible nucleus. The Imaris Measurement Points feature was then used to determine the longest diameter and the perpendicular diameter of the nucleus at the selected Z-step. The mean of these two values was calculated and reported as the average nuclear diameter for DIR neurons. It is important to note that the average diameter values likely represent an underestimate since there was no way to confirm that the cell was imaged at the Z-plane where the nucleus was evenly bisected (i.e., where the nucleus was the largest). The average diameter of DIR pallidal nuclei was 7.95 ± 1.01 µm and did not differ between neurons from

Area X-CORE and SHELL (p = 0.9223; Kolmogorov-Smirnov test). We therefore established a cutoff of 8 µm to separate putative IND pallidal neurons from smaller medium spiny neurons based on nuclear size. While this measurement was established from adult data, we applied the nuclear size cutoff to juveniles because the Alexa 488+ DIR cell size did not differ between adult and juvenile songbirds and the DAPI staining was clearer in adults. Differences in the proportion of large (≥8 um) FoxP2+ nuclei in Area X-CORE and SHELL of adults and juveniles were assessed for statistical significance using a Chi-square test.

Large (≥8 um) FoxP2+ neurons in two juvenile birds were analyzed for overlap with striatal marker DARPP-32 to assess whether these cells were pallidal in nature. We examined 97 FoxP2+ neurons with an average diameter ≥8 µm (putative IND pallidal neurons) across Area X-CORE and SHELL. Each neuron was visually inspected at every Z position for signs of double-label with DARPP-32. To better visualize double-label, figure insets were created using the voxel-based Colocalization feature in Imaris at the Z-step where the FoxP2+ nucleus appeared the largest; white image voxels indicate expression of both FoxP2 and DARPP-32.

3. RESULTS

3.1 Direct DLM-projecting neurons in Area X do not express FoxP2 in adult or juvenile songbirds

We injected DLM with dextran-Alexa 488 in order to retrogradely label thalamus-projecting (DIR) neurons within CORE and SHELL regions of Area X (see Methods; Fig. 3a, 4a). DAPI staining was used to identify the outline of Area X-CORE (Fig. 3b, 4b); Area X-SHELL was defined conservatively as extending 500 µm from the medial, ventromedial, and ventrolateral edges of Area X-CORE (Iyengar et al., 1999). Our injections revealed a topographically organized pattern of retrograde label in Area X-CORE and Area X-SHELL that was consistent with previous work (Johnson et al., 1995; Luo & Perkel, 1999b; Person et al., 2008) (data not shown). Some injections extended beyond the borders of DLM, labeling neurons outside of Area X-CORE and SHELL; we did not include these neurons in our analysis. The precise borders of Area X-CORE were poorly defined in some sections, and some retrogradely-labeled neurons were located very close to the CORE-SHELL border. In these cases, we assigned labeled neurons to the border region between Area X-CORE and Area X-SHELL. Table 2 shows the number of DIR DLM-projecting neurons in Area X-CORE, Area X-SHELL, and the border between them in each bird.

We analyzed a total of 469 retrogradely-labeled neurons across four adult male birds. Sections were stained in two series by different antibodies for FoxP2 (anti-FoxP2 16046 or anti-FoxP2 1307, see Methods) (Fig. 3c). Retrogradely-labeled neurons across Area X-CORE and Area X-SHELL (Fig. 3d) were inspected for overlap with FoxP2 (Fig. 3e, f). Of these 469 DLM-projecting neurons, only two neurons in Area X-CORE showed possible colocalization of Alexa 488 (DLM-projecting) and Alexa 594 (FoxP2) labels ($p < 0.0001$, binomial test) (Fig. 3h). The somata and primary dendrites of Area X neurons that projected to DLM were robustly labeled (Fig. 3f). These primary dendrites were aspiny in nature, characteristic of pallidal neurons as described by Reiner et al. (2004). To determine whether the somal size of DIR neurons differed between Area X-CORE versus Area X-SHELL, 100 DIR neurons from the 469 retrogradely-labeled neurons across four adult birds were randomly selected for size measurements. Of these, 54 were in Area X-CORE, 35 were in Area X-SHELL, and 11 were in the border region; the border region neurons were excluded from size analysis because they could not be definitively categorized into either group. The DIR somata in Area X-CORE had an average diameter of 16.29 ± 2.17 µm ($n = 54$). In comparison, somata in Area X-SHELL had an average diameter of 14.39 ± 1.59 µm ($n = 35$), indicating a statistically significant difference between the two regions ($p = 0.0013$; Kolmogorov-Smirnov test) (Fig. 3g). This difference indicates that DIR neurons in Area X-CORE are larger than those in Area X-SHELL.

We next examined whether the absence of FoxP2 expression in adult DLM-projecting DIR neurons persisted in juvenile zebra finches ($n = 3$). Because qualitative examination in adults revealed that anti-FoxP2 16046 produced a higher incidence of labeled cells than anti-FoxP2 1307, we examined only sections stained with anti-FoxP2 16046 in our juvenile study (Fig. 4c). Retrogradely-labeled cells (Fig. 4d) were analyzed for FoxP2 co-expression (Fig. 4e, f). This analysis included 87 DIR DLM-projecting cells: 38 in Area X-CORE, 26 in Area X-SHELL, and 23 in the border region between CORE and SHELL (Table 2). The size of DLM-projecting somata in Area X-CORE of juveniles (17.05 ± 2.28 µm, $n = 38$) was larger than the somata in Area X-SHELL of juveniles (15.13 ± 2.28 µm, $n = 26$) (Fig. 4g). Like adults, this size difference in retrogradely-labeled neurons was statistically significant ($p = 0.0263$; Kolmogorov-Smirnov test). The size of DIR neurons in juvenile Area X-CORE did not differ compared to adult Area X-CORE ($p = 0.1385$; Kolmogorov-Smirnov test), nor did juvenile Area X-SHELL DIR neuron size differ from those in adult Area X-SHELL ($p = 0.1623$; Kolmogorov-Smirnov test). None of these juvenile DIR neurons showed any expression of FoxP2 (Fig. 4h). Together, these data show that DIR Area X→DLM projection neurons do not express FoxP2 in either adult or juvenile zebra finches.

3.2 FoxP2+ nuclei vary in size and intensity

FoxP2+ nuclei in Area X exhibited a range of sizes in both adult (n = 3) and juvenile birds (n = 2) (Fig. 5a, c). Frequency histograms of size across all FoxP2+ nuclei revealed a continuous, positively skewed distribution for adults and juveniles within both Area X-CORE and Area X-SHELL (Fig. 5b). In Area X-CORE, the average diameter of FoxP2-labeled nuclei ranged from 3.02 µm to 9.97 µm in adults and 3.21 to 10.14 µm in juveniles (Fig. 5b). In Area X-SHELL, the average diameter of labeled nuclei ranged from 3.21 µm to 9.61 µm in adults and 3.46 µm to 10.02 µm in juveniles (Fig. 5b). Thus, FoxP2 was expressed across a similar, continuous distribution of nuclear sizes in CORE and SHELL regions of both juveniles and adults.

FoxP2 is highly expressed in medium spiny neurons of Area X (Haesler et al., 2004; Xiao et al., 2021); however, snRNA-seq analysis by Xiao et. al (2021) showed that FoxP2 is also expressed in other cell types, including pallidal-like neurons. Pallidal cells in the Medial Striatum of songbirds, including Area X, are larger than striatal medium spiny neurons (Luo & Perkel, 1999b; Reiner et al., 2004), as is true in mammals. Reiner et al. (2004) previously reported that DLM-projecting pallidal neurons in zebra finches had average somal diameters of 12.4 ± 1.8 µm. In contrast, they found that the somata of medium spiny neurons, marked by the striatal cytoplasmic marker DARPP-32, had a diameter of 7.1 ± 1.1 µm. Interestingly, we did not observe a bimodal distribution in size suggested by this difference in diameter between medium spiny neurons and pallidal neurons (Fig. 5b). This may be due to the fact that FoxP2 is also expressed in some types of interneurons as well as oligodendrocytes in the avian brain (Xiao et al., 2021). We reasoned that most of the smaller FoxP2+ neurons corresponded to medium spiny neurons (Fig. 5a, c, white arrows), while the sparsely distributed larger FoxP2+ neurons corresponded to IND pallidal neurons (Fig. 5a, c, white arrowheads).

To gauge whether large FoxP2+ cells belonged to a distinct subpopulation, we first determined the nuclear size of DLM-projecting pallidal neurons (see Methods). This analysis indicated that the nuclei of DIR DLM-projecting neurons had an average diameter of 7.95 ± 1.01 µm (n = 50 neurons). We therefore established 8 µm as a cutoff for the average nuclear diameter of a putative FoxP2+ indirect pallidal neuron. In Area X-CORE of adults, 97.42% of FoxP2+ nuclei had an average diameter <8 µm (referred to as “small FoxP2+ cells”); the average diameter of these nuclei was 5.38 ± 0.97 µm (Table 3). In Area X-SHELL, small FoxP2+ nuclei accounted for 97.39% of the total cell count, with a mean diameter of 5.48 ± 0.99 µm (Table 3). In juveniles, small FoxP2+ nuclei comprised 97.30% of Area X-CORE, with a

mean diameter of 5.88 ± 1.03 µm. In juvenile Area X-SHELL, 94.25% of the total cell count were small FoxP2+ cells; the mean diameter of these nuclei was 5.73 ± 1.14 µm (Table 3).

We next analyzed the nuclear size of large FoxP2+ cells – a putative population of IND pallidal neurons. In adult zebra finches, 2.58% of FoxP2+ nuclei in Area X-CORE had an average diameter ≥8 µm (referred to as "large FoxP2+ cells"), with a mean diameter of 8.52 ± 0.48 µm (Table 3). In adult Area X-SHELL, 2.61% of FoxP2+ nuclei were large (8.34 ± 0.38 µm). The difference in size between the large FoxP2+ nuclei of adult Area X-CORE and Area X-SHELL was marginally significant ($p = 0.0543$; Kolmogorov-Smirnov test), but the proportion of large FoxP2+ nuclei did not differ between the CORE and SHELL subregions ($p = 0.9573$; Chi-square test).

In juvenile songbirds, 2.70% and 5.75% of FoxP2+ nuclei were categorized as large (≥8 µm) in Area X-CORE and Area X-SHELL, respectively. The higher proportion of large FoxP2+ nuclei in juvenile Area X-SHELL compared to juvenile Area X-CORE was statistically significant ($p = 0.0001$; Chi-square test). Despite the proportional difference, the diameters of the large FoxP2+ nuclei in juveniles did not differ between Area X-CORE (8.56 ± 0.49 µm) and Area X-SHELL (8.53 ± 0.47 µm) ($p = 0.3346$; Kolmogorov-Smirnov test).

While the proportion of large FoxP2+ nuclei did not differ across the adult and juvenile groups in Area X-CORE ($p = 0.7895$; Chi-square test), Area X-SHELL of juveniles contained a greater proportion of large FoxP2+ nuclei compared to adult Area X-SHELL ($p = 0.0001$; Chi-square test), suggesting a developmental difference in the cellular makeup of this region. Additionally, nuclear size did not differ between large FoxP2+ nuclei in adult versus juvenile Area X-CORE ($p = 0.5441$; Kolmogorov-Smirnov test) or between adult versus juvenile Area X-SHELL ($p = 0.1705$; Kolmogorov-Smirnov test).

Interestingly, our qualitative observations revealed that these large nuclei were generally more intensely stained for FoxP2 than their smaller counterparts in both adults and juveniles (Fig. 5a, 5c). This observation aligns with data from Thompson et al. (2013) and Kosubek-Langer and Scharff (2020), which showed a bimodal distribution of relatively larger intensely-stained FoxP2+ neurons and relatively smaller weakly-stained FoxP2+ neurons in Area X.

3.3 Most large FoxP2+ neurons do not express DARPP-32

In order to investigate whether the larger FoxP2+ neurons were pallidal in nature, we examined the expression of a striatal spiny neuron marker, DARPP-32, in two juvenile songbirds. DLM-projecting cells were never co-labeled with DARPP-32 in Area X-CORE or

Area X-SHELL (Fig. 6a), confirming the pallidal identity of DIR cells. Therefore, if larger FoxP2+ neurons belong to an indirect pallidal class, we expected to observe a similar lack of colocalization with DARPP-32 expression. We analyzed a total of 97 large FoxP2+ neurons with an average diameter ≥8 µm across both Area X-CORE and Area X-SHELL in juveniles. Nuclear FoxP2 staining (red) was inspected for overlap with cytoplasmic DARPP-32 staining (magenta) (Fig. 6b, c). The majority of large FoxP2+ neurons did not express DARPP-32 in both Area-X CORE (65%) and Area X-SHELL (69%); two examples from Area X-CORE are marked by white arrowheads in Figure 6b. The majority of smaller neurons expressed both FoxP2 and DARPP-32 and are likely medium spiny neurons (Fig. 6b, white arrows); the insets depict the colocalization of both proteins in white (see Methods).

Surprisingly, a substantial number of large neurons co-expressed FoxP2 and DARPP-32 in both CORE and SHELL regions of Area X. Figure 6c shows a large neuron in Area X-SHELL that expressed both FoxP2 nuclear staining and DARPP-32 cytoplasmic staining (white arrowhead; inset depicts colocalization in white). Thirty-five percent (17/49) of large FoxP2+ neurons were double-labeled in Area X-CORE and 31% (15/48) were double-labeled in Area X-SHELL in these two birds (Fig. 6d). Interestingly, when neurons in Area X-CORE that had a slightly larger average diameter (≥8.5 µm, n = 22) were selectively examined, only four expressed both FoxP2 and DARPP-32 (8%). Likewise, among neurons in Area X-SHELL with an average diameter ≥8.5 µm (n = 21), only four expressed both DARPP-32 and FoxP2 (8%).

As indicated above, DARPP-32 labeled the majority of smaller FoxP2+ neurons, consistent with an identity of striatal spiny neurons. In both Area X-CORE and SHELL, we noticed that the FoxP2+ nuclei of these smaller double-labeled neurons took up a large percentage of the cytoplasm labeled by DARPP-32, examples of which can be seen in the insets of Figures 6b and 6c (white arrows). These observations conform to the report of Ouimet et al. (1998) that DARPP-32+ medium-sized spiny neurons of rat striatum have scant cytoplasm. Qualitative inspection also suggested that the nuclei of large FoxP2+/DARPP-32+ cells (possible IND neurons) in Area X-CORE and SHELL follow a similar pattern by taking up a large percentage of the cytoplasm. In Figure 6c, the inset of the large FoxP2+ neuron (white arrowhead) shows that the nuclear FoxP2 staining takes up a large percentage of the cytoplasmic DARPP-32 staining, as seen by the white pixels indicating colocalization.

Conversely, when we examined DIR retrogradely-labeled neurons, we observed that the DAPI+ nuclei encompassed a considerably smaller percentage of the soma. This observation was consistent across both Area X-CORE and SHELL regions. Figure 7 shows a DIR neuron in

Area X-CORE in which the DAPI+ nucleus (blue) is surrounded by relatively more cytoplasm (green) compared to Figure 6c (inset, white arrowhead). An adjacent FoxP2+ nucleus may represent an interneuron or a medium spiny neuron. These observations suggest that DIR and IND pallidal cells have a similar nuclear size but vary in the percentage of the soma that their nuclei encompass. DIR neurons may have a larger amount of cytoplasm in order to support a longer axon, and/or other features.

4. DISCUSSION

Vocal learning is mediated in part by two parallel, topographically organized cortico-basal ganglia circuits, CORE and SHELL, that form reentrant loops. Area X sends inhibitory projections to the thalamic nucleus DLM, with Area X-CORE projecting to the dorsolateral subregion of DLM (DLMdl) and Area X-SHELL projecting to the ventromedial subregion of DLM (DLMvm) (Bottjer et al., 1989; Iyengar et al., 1999; Johnson et al., 1995; Person et al., 2008). DLMdl and DLMvm project to LMAN-CORE and LMAN-SHELL respectively, forming a recurrent pathway (Iyengar et al., 1999; Johnson et al., 1995; Luo et al., 2001). Thus, DLM receives input from independent CORE and SHELL pathways as well as convergent input from AId (Bottjer et al., 2000; Foster, Mehta, & Bottjer, 1997). In addition, Area X receives cerebellar inputs via thalamic nuclei adjacent to DLM (Nicholson, Roberts, & Sober, 2018; Person et al., 2008; Pidoux, Le Blanc, Levenes, & Leblois, 2018). Given the complexity of these connections, it remains unclear how motor production and vocal evaluation information converge (Iyengar et al., 1999; Johnson & Bottjer, 1992; Johnson et al., 1995; Paterson & Bottjer, 2017). Our goal in this study was to elucidate specific patterns of connectivity underlying how vocal information is conveyed from Area X to DLM. A prior study using snRNA-seq showed that pallidal neurons in Area X express either FoxP2 or PENK (the precursor to enkephalin), but not both (Xiao et al., 2021). Given that enkephalin is the neurotransmitter of DIR DLM-projecting neurons (Carrillo & Doupe, 2004), this distinction suggested the hypothesis that DLM-projecting pallidal cells are FoxP2-/PENK+, while non-projecting pallidal cells are FoxP2+/PENK-. In this study, we tested FoxP2 expression as a possible marker for direct versus indirect pallidal neurons in Area X as a first step to distinguish how information may be differently conveyed via these two pathways from Area X→DLM.

Consistent with this hypothesis, we found that DIR DLM-projecting neurons in Area X-CORE and Area X-SHELL of both adult and juvenile songbirds consistently lacked expression of FoxP2. Neurons that did express FoxP2 exhibited various sizes and intensities in both

CORE and SHELL regions of Area X. Qualitative inspection revealed a subpopulation of FoxP2+ neurons that were larger and more intensely stained, consistent with findings from Thompson et al. (2013) and Kosubek-Langer and Scharff (2020). Coupled with the results from Xiao et al. (2021) regarding a lack of colocalization between FoxP2 and PENK in Area X, this pattern of results suggests that the larger, more intense FoxP2+ neurons represent a class of indirect pallidal neurons (Farries et al., 2005), while the smaller neurons represent striatal and/or other types of neurons.

In order to test whether these larger FoxP2+ (putative IND) neurons had a pallidal identity, we first measured the diameter of nuclei in DIR DLM-projecting neurons (a known pallidal population). These measurements suggested 8 µm as a cutoff estimate for the nuclear diameter of indirect FoxP2+ pallidal neurons. Surprisingly, we discovered that 32/97 (33%) large (≥8 µm diameter) FoxP2+ neurons expressed the striatal spiny neuron marker DARPP-32. We found that increasing the size of our nuclear cutoff so as to include a slightly larger class of FoxP2+ neurons (≥8.5 µm diameter) greatly reduced the incidence of cells that also expressed DARPP-32, suggesting perhaps that most IND pallidal neurons do not express DARPP-32, or that diverse classes of pallidal cells have a larger range of nuclear size compared to DIR pallidal cells. Our estimate of a threshold for pallidal neuron size may have been low (see Methods); if so that would lend credence to the idea that large FoxP2+ neurons do not express DARPP-32. DARPP-32 is not expressed in pallidal neurons of rodents or pigeons (Anderson & Reiner, 1991; Reiner et al., 1998). In addition, no previous papers have reported the expression of DARPP-32 in larger neurons of rodent basal ganglia to our knowledge. FoxP2 does not colocalize with markers for choline acetyltransferase (ChAT), nitric oxide (nNOS/SS/NPY), or parvalbumin (PV) interneurons in Area X (Haesler et al., 2004). DARPP-32 is also not detectable in cholinergic, PV+, or NPY+ striatal interneurons of rat or pigeon (Anderson & Reiner, 1991; Reiner et al., 1998). However, the snRNA-seq analysis of Xiao et al. (2021) in adult Area X indicated that FoxP2 is expressed at low levels in interneurons (type unknown), oligodendrocytes, and endothelial cells, and that DARPP-32 (PPP1R1B) is expressed at a low level in some pallidal neurons. This latter finding is consistent with our observation of DARPP-32 and FOXP2 co-localizing to a subset of pallidal neurons in juvenile birds.

FoxP2 and DARPP-32 may colocalize in a specific subclass of pallidal neurons only in juvenile birds and could represent a transient feature of vocal learning. Haesler et al. (2004) reported developmental increases in the expression of FoxP2 within Area X that were highest in juvenile zebra finches between 35 and 50 dph, which corresponds to the age range of our

juvenile birds (~45 dph). This age range includes early stages of sensorimotor integration when birds are learning to imitate a memorized tutor song. Increased co-expression of FoxP2 and DARPP-32 may occur within IND pallidal neurons only during this period of vocal learning. Because we did not examine the expression of DARPP-32 in adult birds, this remains an interesting future question. DARPP-32 is a phosphoprotein that is coupled to multiple receptors, including D1/D5 receptors, D2 and adenosine A2a receptors, and NMDA receptors (Blank, 1997; Langley, Bergson, Greengard, & Ouimet, 1997; Yger & Girault, 2011). In striatal tissue, DARPP-32 is necessary for the cAMP-dependent enhancement of NMDA responses (Blank, 1997). Pallidal neurons in Area X are known to receive direct glutamatergic projections from both HVC and LMAN (Farries et al., 2005). Although it is not known whether these cortical projections include an NMDAR-mediated component, NMDA responses are ubiquitous in projections from DLM to LMAN and from HVC and LMAN to RA (Bottjer, 2005; Bottjer, Brady, & Walsh, 1998; Mooney & Konishi, 1991; Stark & Perkel, 1999). It is also not known whether pallidal neurons in Area X receive direct dopaminergic inputs, although DA projections to pallidal cells occur in primates and rodents (Eid & Parent, 2016; Gauthier, Parent, Levesque, & Parent, 1999; Lindvall & Bjorklund, 1979). One intriguing possibility is that DARPP-32 may help to regulate interactions between glutamatergic and dopaminergic afferents by regulating the enhancement of NMDA responses (Blank, 1997).

The growing complexity of cell types and connections in basal ganglia generally (Arber & Costa, 2022; Bostan, Dum, & Strick, 2018; Hegeman, Hong, Hernandez, & Chan, 2016; Oorschot, 2016; Soares-Cunha, Coimbra, Sousa, & Rodrigues, 2016), as well as the combined presence of spiny neurons, pallidal cells, interneurons, and possibly other neuronal cell types within Medial Striatum of avian brain, offer multiple possibilities for the identity of large FoxP2+/DARPP-32+ neurons in Area X. Mammalian GPe contains a heterogeneous assortment of neurons with projections to diverse targets (Hegeman et al., 2016), suggesting that Area X may also contain multiple subclasses of GPe-like pallidal neurons. Xiao et al. (2021) reported that a cluster identified as pallidal neurons by snRNA-seq expressed high levels of markers for a type of GPe neuron known as arkypallidal (Hegeman et al., 2016), which projects back to striatum in mammals. In accordance with this idea, there are no pallidal projections from Area X to the subthalamic nucleus (STN), and pallidal neurons within Area X seem to make collateral projections onto spiny neurons (Farries et al., 2005; Gale & Perkel, 2010). Further characterization based on additional molecular markers combined with patterns of connectivity in both juvenile and adult zebra finches are necessary to distinguish whether the non-projecting pallidal cells of CORE and SHELL regions of Area X contain distinct subclasses.

Overall, our findings indicate that FoxP2 staining, along with size measurements, may be used as a marker to distinguish the indirect pallidal neuron population in Area X that forms close contacts with direct DLM-projecting pallidal neurons (Farries et al., 2005). In terms of functional roles, the direct pathway of the basal ganglia increases thalamic activity, whereas the indirect pathway is thought to oppose the DIR pathway to decrease thalamic activity (Alexander & Crutcher, 1990). When self-generated vocal motor output matches the memorized tutor song, the direct pathway may enhance firing in DLM to generate a positive reinforcement signal for "correct" vocal behavior. In contrast, pallidal neurons that receive inputs from spiny neurons in a "traditional" indirect pathway would suppress firing in DLM. In that case, the indirect pathway may be involved in generating a negative reinforcement signal for "incorrect" behavior when vocalizations differ from memorized tutor sounds. However, because some pallidal neurons in Area X receive direct cortical inputs from HVC and LMAN, those excitatory inputs might increase firing rates in a subset of IND neurons, which would decrease firing rates in DIR neurons and thus increase thalamic activity (Farries et al., 2005). Understanding how these pathways connect and process motor skill information within the LMAN→Area X→DLM→LMAN feedback loop will provide insight into what roles the basal ganglia pathways play in vocal learning in songbirds as well as motor learning in humans.

5. REFERENCES

Achiro, J. M., & Bottjer, S. W. (2013). Neural representation of a target auditory memory in a cortico-basal ganglia pathway. *J Neurosci, 33*(36), 14475-14488. doi:10.1523/JNEUROSCI.0710-13.2013

Achiro, J. M., Shen, J., & Bottjer, S. W. (2017). Neural activity in cortico-basal ganglia circuits of juvenile songbirds encodes performance during goal-directed learning. *Elife, 6*. doi:10.7554/eLife.26973

Alexander, G. E., & Crutcher, M. D. (1990). Functional architecture of basal ganglia circuits: neural substrates of parallel processing. *Trends Neurosci, 13*(7), 266-271.

Alvarez-Buylla, A., & Nottebohm, F. (1988). Migration of young neurons in adult avian brain. *Nature, 335*(6188), 353-354.

Anderson, K. D., & Reiner, A. (1991). Immunohistochemical localization of DARPP-32 in striatal projection neurons and striatal interneurons: implications for the localization of D1-like dopamine receptors on different types of striatal neurons. *Brain Resaerch, 568*(1-2), 235-243. doi:10.1016/0006-8993(91)91403-n

Arber, S., & Costa, R. M. (2022). Networking brainstem and basal ganglia circuits for movement. *Nat Rev Neurosci, 23*(6), 342-360. doi:10.1038/s41583-022-00581-w

Aronov, D., Andalman, A. S., & Fee, M. S. (2008). A specialized forebrain circuit for vocal babbling in the juvenile songbird. *Science, 320*(5876), 630-634. doi:320/5876/630 [pii] 10.1126/science.1155140

Blank, R. H. (1997). Assisted reproduction and reproductive rights: the case of in vitro fertilization. *Politics Life Sci, 16*(2), 279-288. doi:10.1017/s0730938400024849

Böhner, J. (1983). Song Learning in the Zebra Finch (Taeniopygia-Guttata) - Selectivity in the Choice of a Tutor and Accuracy of Song Copies. *Animal Behaviour, 31*(Feb), 231-237. doi:Doi 10.1016/S0003-3472(83)80193-6

Böhner, J. (1990). Early acquisition of song in the zebra finch, *Taeniopygia guttata*. *Animal Behaviour, 39*, 369-374.

Bostan, A. C., Dum, R. P., & Strick, P. L. (2018). Functional Anatomy of Basal Ganglia Circuits with the Cerebral Cortex and the Cerebellum. *Prog Neurol Surg, 33*, 50-61. doi:10.1159/000480748

Bottjer, S. W. (2005). Silent synapses in a thalamo-cortical circuit necessary for song learning in zebra finches. *Journal of Neurophysiology, 94*(6), 3698-3707.

Bottjer, S. W., & Altenau, B. (2010). Parallel pathways for vocal learning in basal ganglia of songbirds. *Nat Neurosci, 13*(2), 153-155. doi:10.1038/nn.2472

Bottjer, S. W., & Arnold, A. P. (1986). The ontogeny of bird song: Neural mechanisms of vocal learning. In E. M. Blass (Ed.), *Handbook of Behavioral Neurobiology: Developmental Processes in Psychobiology and Neurobiology* (Vol. 8, pp. 129-161). New York: Plenum.

Bottjer, S. W., Brady, J. D., & Cribbs, B. (2000). Connections of a motor cortical region in zebra finches: relation to pathways for vocal learning. *J Comp Neurol, 420*(2), 244-260.

Bottjer, S. W., Brady, J. D., & Walsh, J. P. (1998). Intrinsic and synaptic properties of neurons in the vocal-control nucleus IMAN from in vitro slice preparations of juvenile and adult zebra finches. *J Neurobiol, 37*(4), 642-658.

Bottjer, S. W., Halsema, K. A., Brown, S. A., & Miesner, E. A. (1989). Axonal connections of a forebrain nucleus involved with vocal learning in zebra finches. *J Comp Neurol, 279*(2), 312-326.

Bottjer, S. W., Miesner, E. A., & Arnold, A. P. (1984). Forebrain lesions disrupt development but not maintenance of song in passerine birds. *Science, 224*(4651), 901-903.

Campbell, P., Reep, R. L., Stoll, M. L., Ophir, A. G., & Phelps, S. M. (2009). Conservation and diversity of Foxp2 expression in muroid rodents: functional implications. *J Comp Neurol, 512*(1), 84-100. doi:10.1002/cne.21881

Carrillo, G. D., & Doupe, A. J. (2004). Is the songbird Area X striatal, pallidal, or both? An anatomical study. *J Comp Neurol, 473*(3), 415-437.

Catchpole, C., & Slater, P. J. B. (1995). *Bird song : biological themes and variations*. Cambridge England ;: New York, NY Cambridge University Press.

Clayton, N. S. (1987). Song Learning in Cross-Fostered Zebra Finches - a Reexamination of the Sensitive Phase. *Behaviour, 102*, 67-81.

den Hoed, J., & Fisher, S. E. (2020). Genetic pathways involved in human speech disorders. *Curr Opin Genet Dev, 65*, 103-111. doi:10.1016/j.gde.2020.05.012

Doupe, A. J., & Kuhl, P. K. (1999). Birdsong and human speech: common themes and mechanisms. *Annual Review of Neuroscience, 22*, 567-631.

Durstewitz, D., Kroner, S., Hemmings, H. C., Jr., & Gunturkun, O. (1998). The dopaminergic innervation of the pigeon telencephalon: distribution of DARPP-32 and co-occurrence with glutamate decarboxylase and tyrosine hydroxylase. *Neuroscience, 83*(3), 763-779. doi:10.1016/s0306-4522(97)00450-8

Eales, L. A. (1985). Song learning in zebra finches - some effects of song model availability on what is learnt and when *Animal Behaviour, 33*(NOV), 1293-1300.

Eid, L., & Parent, M. (2016). Chemical anatomy of pallidal afferents in primates. *Brain Struct Funct, 221*(9), 4291-4317. doi:10.1007/s00429-016-1216-y

Farries, M. A., Ding, L., & Perkel, D. J. (2005). Evidence for "direct" and "indirect" pathways through the song system basal ganglia. *J Comp Neurol, 484*(1), 93-104.

Foster, E. F., Mehta, R. P., & Bottjer, S. W. (1997). Axonal connections of the medial magnocellular nucleus of the anterior neostriatum in zebra finches. *J Comp Neurol, 382*(3), 364-381.

Gale, S. D., & Perkel, D. J. (2010). Anatomy of a songbird basal ganglia circuit essential for vocal learning and plasticity. *J Chem Neuroanat, 39*(2), 124-131. doi:10.1016/j.jchemneu.2009.07.003

Gale, S. D., Person, A. L., & Perkel, D. J. (2008). A novel basal ganglia pathway forms a loop linking a vocal learning circuit with its dopaminergic input. *J Comp Neurol, 508*(5), 824-839. doi:10.1002/cne.21700

Gauthier, J., Parent, M., Levesque, M., & Parent, A. (1999). The axonal arborization of single nigrostriatal neurons in rats. *Brain Resaerch, 834*(1-2), 228-232. doi:10.1016/s0006-8993(99)01573-5

Goldberg, J. H., Adler, A., Bergman, H., & Fee, M. S. (2010). Singing-related neural activity distinguishes two putative pallidal cell types in the songbird basal ganglia: comparison to the primate internal and external pallidal segments. *J Neurosci, 30*(20), 7088-7098. doi:10.1523/JNEUROSCI.0168-10.2010

Graybiel, A. M. (2008). Habits, rituals, and the evaluative brain. *Annual Review of Neuroscience, 31*, 359-387. doi:10.1146/annurev.neuro.29.051605.112851

Haesler, S., Rochefort, C., Georgi, B., Licznerski, P., Osten, P., & Scharff, C. (2007). Incomplete and inaccurate vocal imitation after knockdown of FoxP2 in songbird basal ganglia nucleus Area X. *PLoS Biol, 5*(12), e321. doi:10.1371/journal.pbio.0050321

Haesler, S., Wada, K., Nshdejan, A., Morrisey, E. E., Lints, T., Jarvis, E. D., & Scharff, C. (2004). FoxP2 expression in avian vocal learners and non-learners. *J Neurosci, 24*(13), 3164-3175. doi:10.1523/JNEUROSCI.4369-03.2004

Hegeman, D. J., Hong, E. S., Hernandez, V. M., & Chan, C. S. (2016). The external globus pallidus: progress and perspectives. *Eur J Neurosci, 43*(10), 1239-1265. doi:10.1111/ejn.13196

Hemmings, H. C., Jr., & Greengard, P. (1986). DARPP-32, a dopamine- and adenosine 3':5'-monophosphate-regulated phosphoprotein: regional, tissue, and phylogenetic distribution. *J Neurosci, 6*(5), 1469-1481. doi:10.1523/JNEUROSCI.06-05-01469.1986

Immelmann, K. (Ed.) (1969). *Song development in the zebra finch and other estrildid finches* (Vol. Bird Vocalizations).

Iyengar, S., Viswanathan, S. S., & Bottjer, S. W. (1999). Development of topography within song control circuitry of zebra finches during the sensitive period for song learning. *J Neurosci, 19*(14), 6037-6057.

Johnson, F., & Bottjer, S. W. (1992). Growth and regression of thalamic efferents in the song-control system of male zebra finches. *J Comp Neurol, 326*(3), 442-450.

Johnson, F., Sablan, M. M., & Bottjer, S. W. (1995). Topographic organization of a forebrain pathway involved with vocal learning in zebra finches. *J Comp Neurol, 358*(2), 260-278.

Kosubek-Langer, J., & Scharff, C. (2020). Dynamic FoxP2 levels in male zebra finches are linked to morphology of adult-born Area X medium spiny neurons. *Sci Rep, 10*(1), 4787. doi:10.1038/s41598-020-61740-6

Kubikova, L., Wada, K., & Jarvis, E. D. (2010). Dopamine receptors in a songbird brain. *J Comp Neurol, 518*(6), 741-769. doi:10.1002/cne.22255

Langley, K. C., Bergson, C., Greengard, P., & Ouimet, C. C. (1997). Co-localization of the D1 dopamine receptor in a subset of DARPP-32-containing neurons in rat caudate-putamen. *Neuroscience, 78*(4), 977-983. doi:10.1016/s0306-4522(96)00583-0

Lindvall, O., & Bjorklund, A. (1979). Dopaminergic innervation of the globus pallidus by collaterals from the nigrostriatal pathway. *Brain Resaerch, 172*(1), 169-173. doi:10.1016/0006-8993(79)90907-7

Luo, M., Ding, L., & Perkel, D. J. (2001). An avian basal ganglia pathway essential for vocal learning forms a closed topographic loop. *J Neurosci, 21*(17), 6836-6845.

Luo, M., & Perkel, D. J. (1999a). A GABAergic, strongly inhibitory projection to a thalamic nucleus in the zebra finch song system. *J Neurosci, 19*(15), 6700-6711.

Luo, M., & Perkel, D. J. (1999b). Long-range GABAergic projection in a circuit essential for vocal learning. *J Comp Neurol, 403*(1), 68-84.

Mann, N. I., & Slater, P. J. B. (1995). Song Tutor Choice by Zebra Finches in Aviaries. *Animal Behaviour, 49*(3), 811-820.

Mooney, R., & Konishi, M. (1991). Two distinct inputs to an avian song nucleu activate different glutamate receptor subtypes on individual neurons *Proceedings of the National Academy of Sciences of the United States of America, 88*(10), 4075-4079.

Nicholson, D. A., Roberts, T. F., & Sober, S. J. (2018). Thalamostriatal and cerebellothalamic pathways in a songbird, the Bengalese finch. *J Comp Neurol, 526*(9), 1550-1570. doi:10.1002/cne.24428

Nixdorf-Bergweiler, B. E., Lips, M. B., & Heinemann, U. (1995). Electrophysiological and morphological evidence for a new projection of LMAN-neurones towards area X. *Neuroreport, 6*(13), 1729-1732.

Nottebohm, F., Stokes, T. M., & Leonard, C. M. (1976). Central control of song in the canary, Serinus canarius. *J Comp Neurol, 165*(4), 457-486.

Oorschot, D. E. (2016). Cell types in the different nuclei of the basal ganglia In *Handbook of Behavioral Neuroscience.* (Vol. 24, pp. 99-117.): Elsevier.

Ouimet, C. C., Langley-Gullion, K. C., & Greengard, P. (1998). Quantitative immunocytochemistry of DARPP-32-expressing neurons in the rat caudatoputamen. *Brain Resaerch, 808*(1), 8-12. doi:10.1016/s0006-8993(98)00724-0

Paterson, A. K., & Bottjer, S. W. (2017). Cortical inter-hemispheric circuits for multimodal vocal learning in songbirds. *J Comp Neurol, 525*(15), 3312-3340. doi:10.1002/cne.24280

Person, A. L., Gale, S. D., Farries, M. A., & Perkel, D. J. (2008). Organization of the songbird basal ganglia, including area X. *J Comp Neurol, 508*(5), 840-866. doi:10.1002/cne.21699

Pidoux, L., Le Blanc, P., Levenes, C., & Leblois, A. (2018). A subcortical circuit linking the cerebellum to the basal ganglia engaged in vocal learning. *Elife, 7*. doi:10.7554/eLife.32167

Redgrave, P., Rodriguez, M., Smith, Y., Rodriguez-Oroz, M. C., Lehericy, S., Bergman, H., . . . Obeso, J. A. (2010). Goal-directed and habitual control in the basal ganglia: implications for Parkinson's disease. *Nat Rev Neurosci, 11*(11), 760-772. doi:10.1038/nrn2915

Reiner, A., Laverghetta, A. V., Meade, C. A., Cuthbertson, S. L., & Bottjer, S. W. (2004). An immunohistochemical and pathway tracing study of the striatopallidal organization of area X in the male zebra finch. *J Comp Neurol, 469*(2), 239-261.

Reiner, A., Perera, M., Paullus, R., & Medina, L. (1998). Immunohistochemical localization of DARPP32 in striatal projection neurons and striatal interneurons in pigeons. *J Chem Neuroanat, 16*(1), 17-33. doi:10.1016/s0891-0618(98)00056-8

Roper, A., & Zann, R. (2006). The onset of song learning and song tutor selection in fledgling zebra finches. *Ethology, 112*(5), 458-470. doi:DOI 10.1111/j.1439-0310.2005.01169.x

Sanchez-Valpuesta, M., Suzuki, Y., Shibata, Y., Toji, N., Ji, Y., Afrin, N., . . . Wada, K. (2019). Corticobasal ganglia projecting neurons are required for juvenile vocal learning but not for adult vocal plasticity in songbirds. *Proceedings of the National Academy of Sciences of the United States of America, 116*(45), 22833-22843. doi:10.1073/pnas.1913575116

Scharff, C., & Nottebohm, F. (1991). A comparative study of the behavioral deficits following lesions of various parts of the zebra finch song system: implications for vocal learning. *J Neurosci, 11*(9), 2896-2913.

Shi, Z., Piccus, Z., Zhang, X., Yang, H., Jarrell, H., Ding, Y., . . . Li, X. (2018). miR-9 regulates basal ganglia-dependent developmental vocal learning and adult vocal performance in songbirds. *Elife, 7*. doi:10.7554/eLife.29087

Singh, U. A., & Iyengar, S. (2019). The expression of DARPP-32 in adult male zebra finches (Taenopygia guttata). *Brain Struct Funct, 224*(8), 2939-2972. doi:10.1007/s00429-019-01947-0

Soares-Cunha, C., Coimbra, B., Sousa, N., & Rodrigues, A. J. (2016). Reappraising striatal D1- and D2-neurons in reward and aversion. *Neurosci Biobehav Rev, 68*, 370-386. doi:10.1016/j.neubiorev.2016.05.021

Sohrabji, F., Nordeen, E. J., & Nordeen, K. W. (1990). Selective impairment of song learning following lesions of a forebrain nucleus in the juvenile zebra finch. *Behav Neural Biol, 53*(1), 51-63.

Stark, L. L., & Perkel, D. J. (1999). Two-stage, input-specific synaptic maturation in a nucleus essential for vocal production in the zebra finch. *J Neurosci, 19*(20), 9107-9116.

Thompson, C. K., Schwabe, F., Schoof, A., Mendoza, E., Gampe, J., Rochefort, C., & Scharff, C. (2013). Young and intense: FoxP2 immunoreactivity in Area X varies with age, song stereotypy, and singing in male zebra finches. *Front Neural Circuits, 7*, 24. doi:10.3389/fncir.2013.00024

Vates, G. E., & Nottebohm, F. (1995). Feedback circuitry within a song-learning pathway. *Proceedings of the National Academy of Sciences of the United States of America, 92*(11), 5139-5143.

Xiao, L., Merullo, D. P., Koch, T. M. I., Cao, M., Co, M., Kulkarni, A., . . . Roberts, T. F. (2021). Expression of FoxP2 in the basal ganglia regulates vocal motor sequences in the adult songbird. *Nat Commun, 12*(1), 2617. doi:10.1038/s41467-021-22918-2

Yger, M., & Girault, J. A. (2011). DARPP-32, Jack of All Trades… Master of Which? *Front Behav Neurosci, 5*, 56. doi:10.3389/fnbeh.2011.00056

Yin, H. H., & Knowlton, B. J. (2006). The role of the basal ganglia in habit formation. *Nat Rev Neurosci, 7*(6), 464-476. doi:10.1038/nrn1919

FIGURE LEGENDS

Figure 1. Schematics of cortico-basal ganglia circuits in zebra finches. (a) Simplified schematic of cortico-basal ganglia circuits that mediate vocal learning in songbirds. The pathway from LMAN→Area X→DLM comprises independent parallel loops. (b) Schematic of putative direct (DIR) and indirect (IND) pathways from Area X to the thalamus (DLM). Abbreviations: RA, robust nucleus of the arcopallium; AId, dorsal intermediate arcopallium; LMAN, lateral magnocellular nucleus of the anterior nidopallium; DLM, medial portion of the dorsolateral anterior thalamic nucleus, HVC, high vocal center; MSN, medium spiny neuron.

Figure 2. Surfaces auto-detection feature was used to measure size of FoxP2+ nuclei. Confocal image depicting Imaris Surfaces model (shown in white outline) around FoxP2+ nuclei. See text for further details.

Figure 3. DIR neurons in Area X of adult zebra finches do not express FoxP2. (a) Example of fluorescent tracer injection into DLM (outlined by dashed line). Injections produced strong retrograde label in Area X-CORE and Area X-SHELL (d-f). Injection site extended beyond the borders of DLM, but we did not analyze labeled neurons outside of the CORE and SHELL regions of Area X (see Methods). (b) In a different bird than (a), DAPI staining outlines Area X-CORE (dashed circle) within Medial Striatum of basal ganglia (white line marks the axon tract PSL, pallial-subpallial lamina, which separates striatum from cortex). (c) Red FoxP2 staining using 16046 antibody and (d) green retrogradely-labeled cells from DLM (Alexa 488) in the same section as (b). Green label in upper left corner of (d) and (e) represents anterograde label in LMAN. (e) Overlay of DAPI, FoxP2, and DLM-projecting (Alexa 488) dyes. (f) Enlarged image of two DIR DLM-projecting neurons in Area X-CORE from a different section than (b-e) demonstrating that red FoxP2 label and green DLM-projecting retrograde label did not colocalize. (g) Box plots showing that the average somal diameter of DIR DLM-projecting neurons in Area X-CORE ($n = 54$) was larger than those in Area X-SHELL ($n = 35$) (*$p = 0.0013$; Kolmogorov-Smirnov test). (h) Bar graph showing that 467/469 DIR neurons in Area X-CORE and SHELL of 4 adult birds did not express FoxP2 ($p < 0.0001$, binomial test).

Figure 4. DIR neurons in Area X of juvenile songbirds do not express FoxP2.

(a) Injection of a fluorescent tracer into DLM (outlined by dashed line) produced strong retrograde label in Area X-CORE and SHELL (d-f). (b) DAPI staining outlines Area X-CORE (dashed circle) within Medial Striatum (the border between striatum and cortex is demarcated by

white line, which corresponds to the axon tract PSL, pallial-subpallial lamina). (c) Red FoxP2 staining using 16046 antibody and (d) green DLM-projecting neurons (Alexa 488) in the same section as (b). (e) Overlay of DAPI, FoxP2, and DLM-projecting dyes. (f) Enlarged image of boxed region in (e) demonstrating that red FoxP2 label and green retrograde label in an Area X-CORE DIR neuron did not colocalize. (g) Box plot showing that the average somal diameter of DIR DLM-projecting neurons in Area X-CORE (n = 38) was larger than those in Area X-SHELL (n = 26) (*p = 0.0263; Kolmogorov-Smirnov test). (h) Bar graph detailing that no DIR neurons in 3 juvenile birds (n = 87) showed FoxP2 expression.

Figure 5. Average diameters of FoxP2+ neurons in Area X-CORE and SHELL revealed continuous, positively skewed size distributions. FoxP2 staining distinguished sparsely distributed large nuclei (white arrowheads) and numerous small nuclei (white arrows) in Area X-CORE of (a) adult and (c) juvenile songbirds. This pattern was also present in Area X-SHELL (not shown). Most small FoxP2+ neurons were less intensely stained and are likely striatal spiny neurons; large intensely stained FoxP2+ neurons represent putative IND pallidal neurons. (b) Histograms showing average diameter of FoxP2+ neurons in Area X-CORE (black, n = 3953) and SHELL (gray, n = 1535) of three adult birds (top) and two juvenile birds (bottom; CORE, black, n = 1814; SHELL, gray, n = 835).

Figure 6. All DIR and most putative IND neurons did not express the striatal marker DARPP-32 in juvenile songbirds. (a) Alexa 488-labeled DIR DLM-projecting neurons (one shown from Area X-CORE) did not colocalize with magenta cytoplasmic DARPP-32 label. (b) Most large (≥8 μm) putative IND FoxP2+ nuclei across both Area X-CORE and SHELL did not express DARPP-32; two examples from Area-X CORE are indicated by white arrowheads. A majority of small (<8 μm) FoxP2+ nuclei expressed DARPP-32 (two examples indicated by white arrows). Insets depict the colocalization of both proteins in white. (c) Some large (≥8 μm) FoxP2+ nuclei expressed DARPP-32 in both CORE and SHELL regions of Area X; white arrowhead indicates a large FoxP2+/DARPP-32+ neuron from Area-X SHELL. An adjacent small (<8 μm; white arrow) FoxP2+ nucleus also expressed DARPP-32. Colocalization insets show that the FoxP2+ nuclei of the putative IND and medium spiny neuron take up a large percentage of the DARPP-32+ cytoplasm. (d) Bar graph detailing the proportion of large FoxP2+ neurons that show DARPP-32 expression in Area X-CORE (17/49 neurons) and Area X-SHELL (15/48 neurons) from two juvenile songbirds.

Figure 7. DLM-projecting DIR pallidal cell and adjacent FoxP2+ neuron have similar DAPI+ nuclear sizes. The nucleus of a green Alexa 488+ retrogradely-labeled cell is defined

by blue DAPI nuclear stain in Area X-CORE of an adult bird. DAPI+ nucleus of DIR neuron encompasses a smaller percentage of the soma in comparison to putative IND large FoxP2+/DARPP-32+ cells (see Fig. 6c); this pattern was also present in Area X-SHELL (not shown). The adjacent red FoxP2+ nucleus may represent an interneuron or a medium spiny neuron.

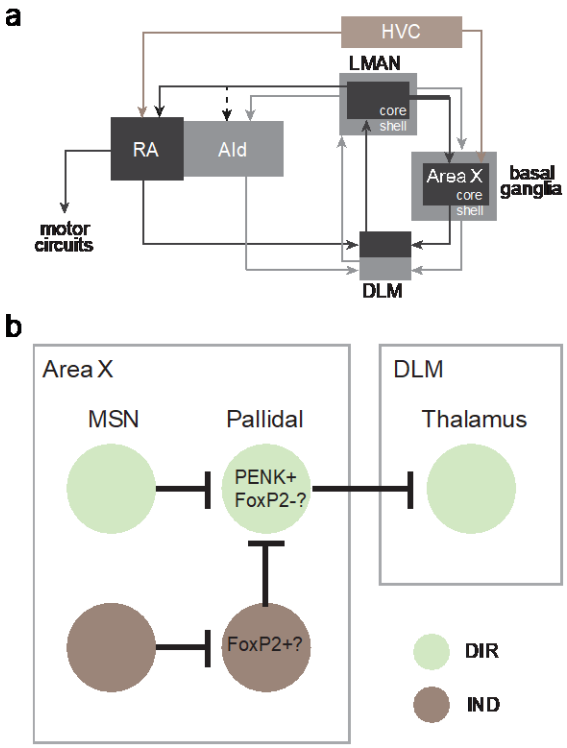

Figure 1. Schematics of cortico-basal ganglia circuits in zebra finches. (a) Simplified schematic of cortico-basal ganglia circuits that mediate vocal learning in songbirds. The pathway from LMAN→Area X→DLM comprises independent parallel loops. (b) Schematic of putative direct (DIR) and indirect (IND) pathways from Area X to the thalamus (DLM). Abbreviations: RA, robust nucleus of the arcopallium; AId, dorsal intermediate arcopallium; LMAN, lateral magnocellular nucleus of the anterior nidopallium; DLM, medial portion of the dorsolateral anterior thalamic nucleus, HVC, high vocal center; MSN, medium spiny neuron.

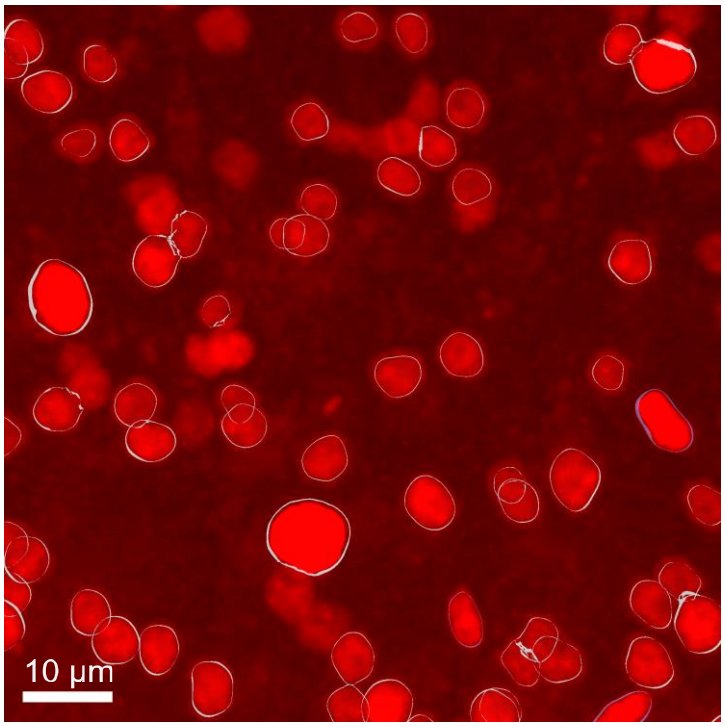

Figure 2. Surfaces auto-detection feature was used to measure size of FoxP2+ nuclei. Confocal image depicting Imaris Surfaces model (shown in white outline) around FoxP2+ nuclei. See text for further details.

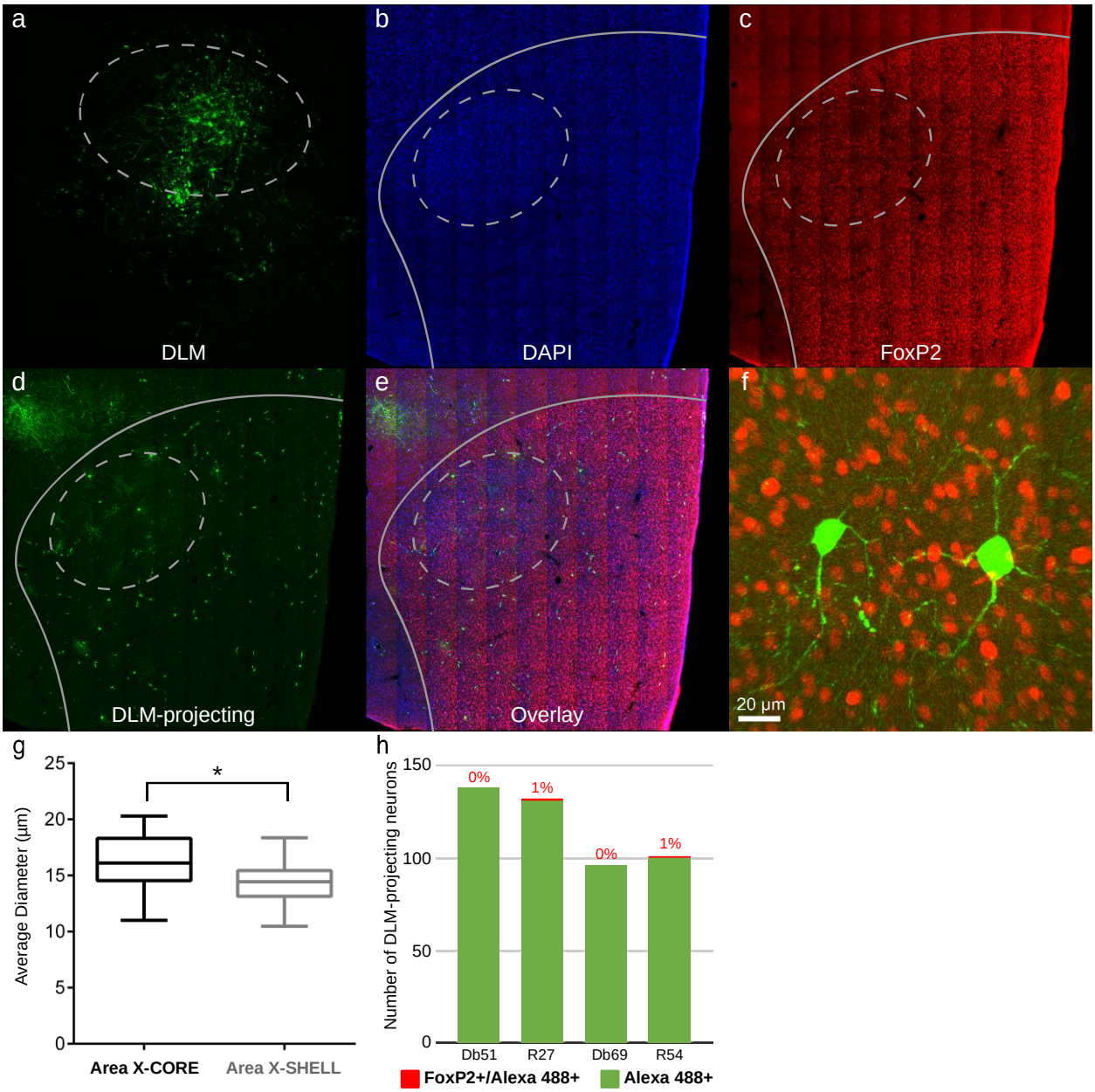

Figure 3. DIR neurons in Area X of adult zebra finches do not express FoxP2.
(a) Example of fluorescent tracer injection into DLM (outlined by dashed line). Injections produced strong retrograde label in Area X-CORE and Area X-SHELL (d-f). Injection site extended beyond the borders of DLM, but we did not analyze labeled neurons outside of the CORE and SHELL regions of Area X (see Methods). (b) In a different bird than (a), DAPI staining outlines Area X-CORE (dashed circle) within Medial Striatum of basal ganglia (white line marks the axon tract PSL, pallial-subpallial lamina, which separates striatum from

cortex). (c) Red FoxP2 staining using 16046 antibody and (d) green retrogradely-labeled cells from DLM (Alexa 488) in the same section as (b). Green label in upper left corner of (d) and (e) represents anterograde label in LMAN. (e) Overlay of DAPI, FoxP2, and DLM-projecting (Alexa 488) dyes. (f) Enlarged image of two DIR DLM-projecting neurons in Area X-CORE from a different section than (b-e) demonstrating that red FoxP2 label and green DLM-projecting retrograde label did not colocalize. (g) Box plots showing that the average somal diameter of DIR DLM-projecting neurons in Area X-CORE ($n = 54$) was larger than those in Area X-SHELL ($n = 35$) (*$p = 0.0013$; Kolmogorov-Smirnov test). (h) Bar graph showing that 467/469 DIR neurons in Area X-CORE and SHELL of 4 adult birds did not express FoxP2 ($p < 0.0001$, binomial test).

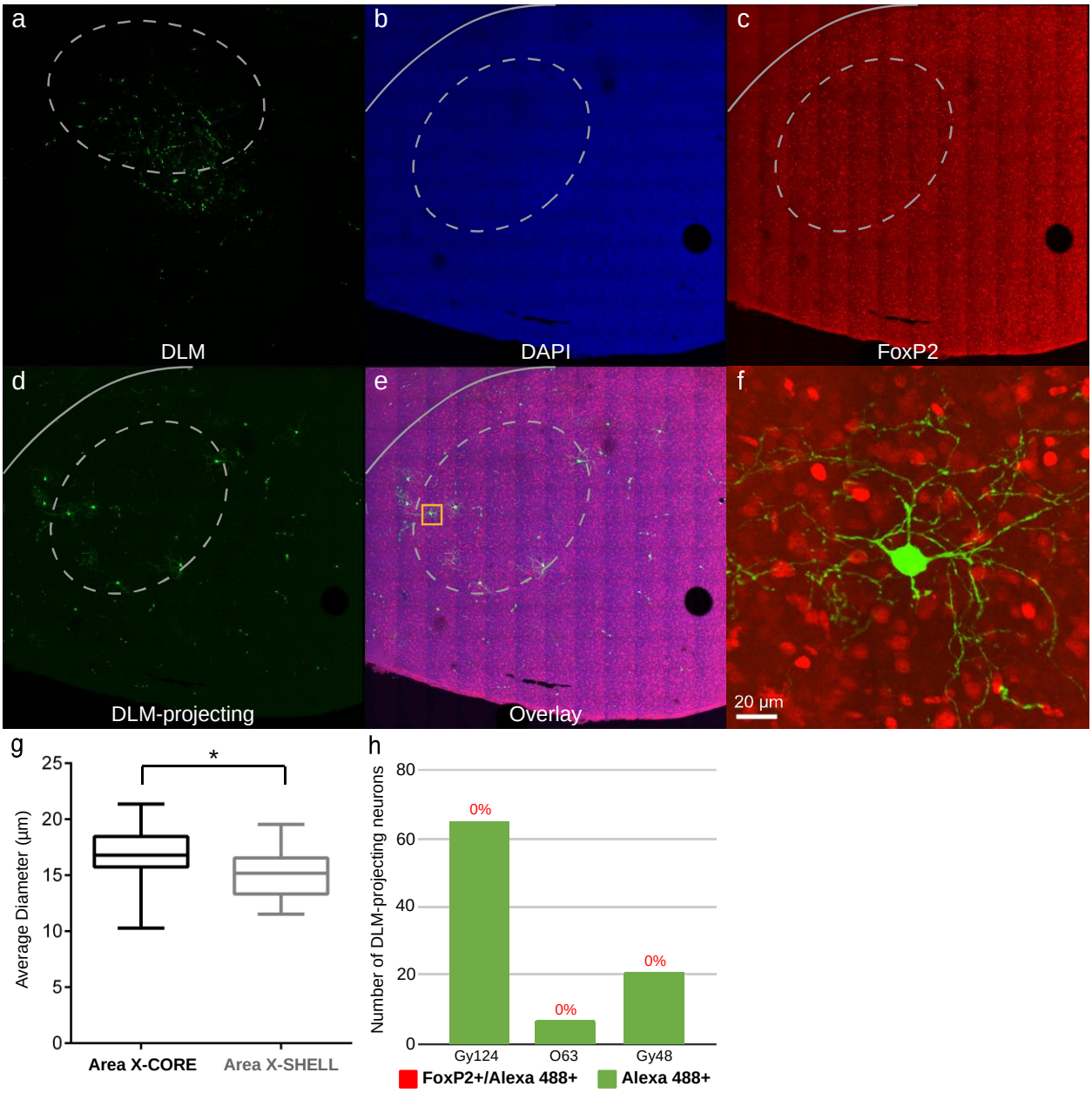

Figure 4. DIR neurons in Area X of juvenile songbirds do not express FoxP2.

(a) Injection of a fluorescent tracer into DLM (outlined by dashed line) produced strong retrograde label in Area X-CORE and SHELL (d-f). (b) DAPI staining outlines Area X-CORE (dashed circle) within Medial Striatum (the border between striatum and cortex is demarcated by white line, which corresponds to the axon tract PSL, pallial-subpallial lamina). (c) Red FoxP2 staining using 16046 antibody and (d) green DLM-projecting neurons (Alexa 488) in the same

section as (b). (e) Overlay of DAPI, FoxP2, and DLM-projecting dyes. (f) Enlarged image of boxed region in (e) demonstrating that red FoxP2 label and green retrograde label in an Area X-CORE DIR neuron did not colocalize. (g) Box plot showing that the average somal diameter of DIR DLM-projecting neurons in Area X-CORE (n = 38) was larger than those in Area X-SHELL (n = 26) (*p = 0.0263; Kolmogorov-Smirnov test). (h) Bar graph detailing that no DIR neurons in 3 juvenile birds (n = 87) showed FoxP2 expression.

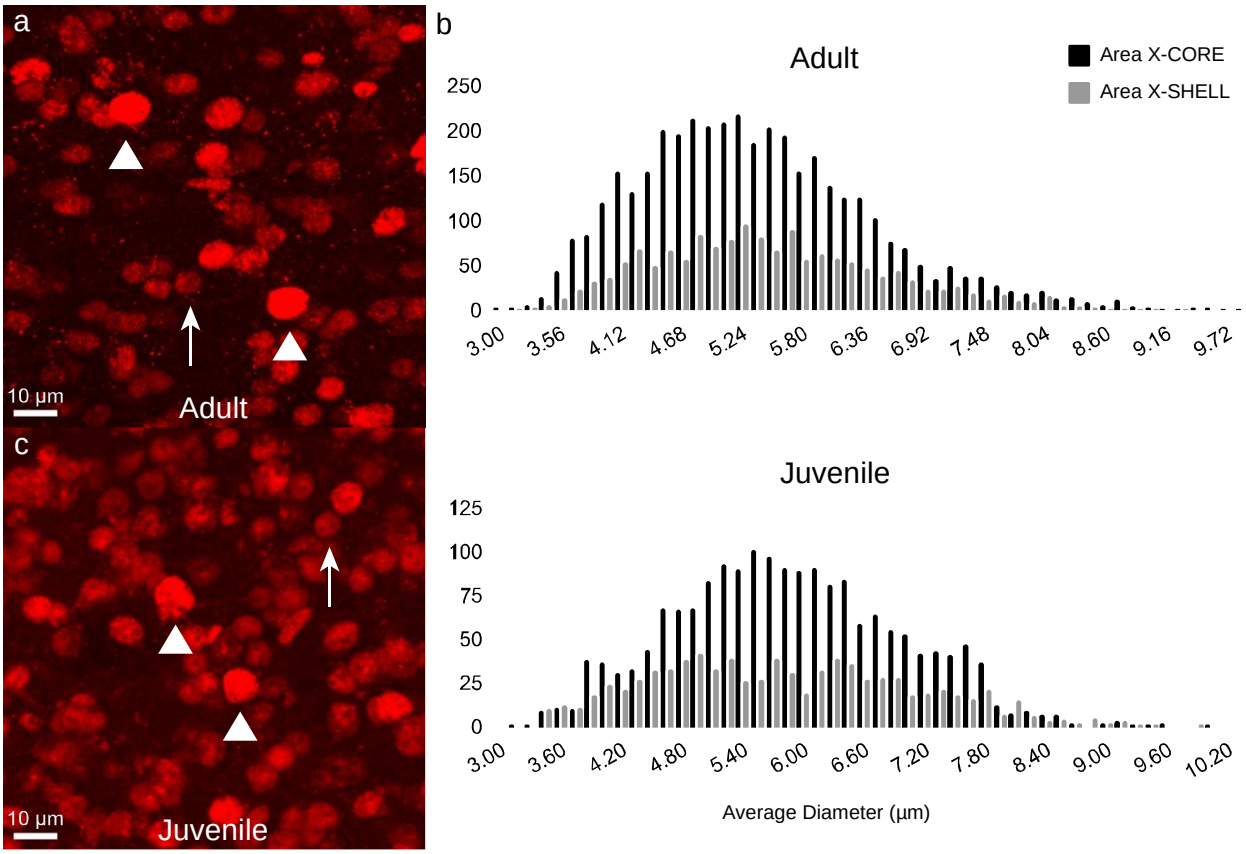

Figure 5. Average diameters of FoxP2+ neurons in Area X-CORE and SHELL revealed continuous, positively skewed size distributions. FoxP2 staining distinguished sparsely distributed large nuclei (white arrowheads) and numerous small nuclei (white arrows) in Area X-CORE of (a) adult and (c) juvenile songbirds. This pattern was also present in Area X-SHELL (not shown). Most small FoxP2+ neurons were less intensely stained and are likely striatal spiny neurons; large intensely stained FoxP2+ neurons represent putative IND pallidal neurons. (b) Histograms showing average diameter of FoxP2+ neurons in Area X-CORE (black, n = 3953) and SHELL (gray, n = 1535) of three adult birds (top) and two juvenile birds (bottom; CORE, black, n = 1814; SHELL, gray, n = 835).

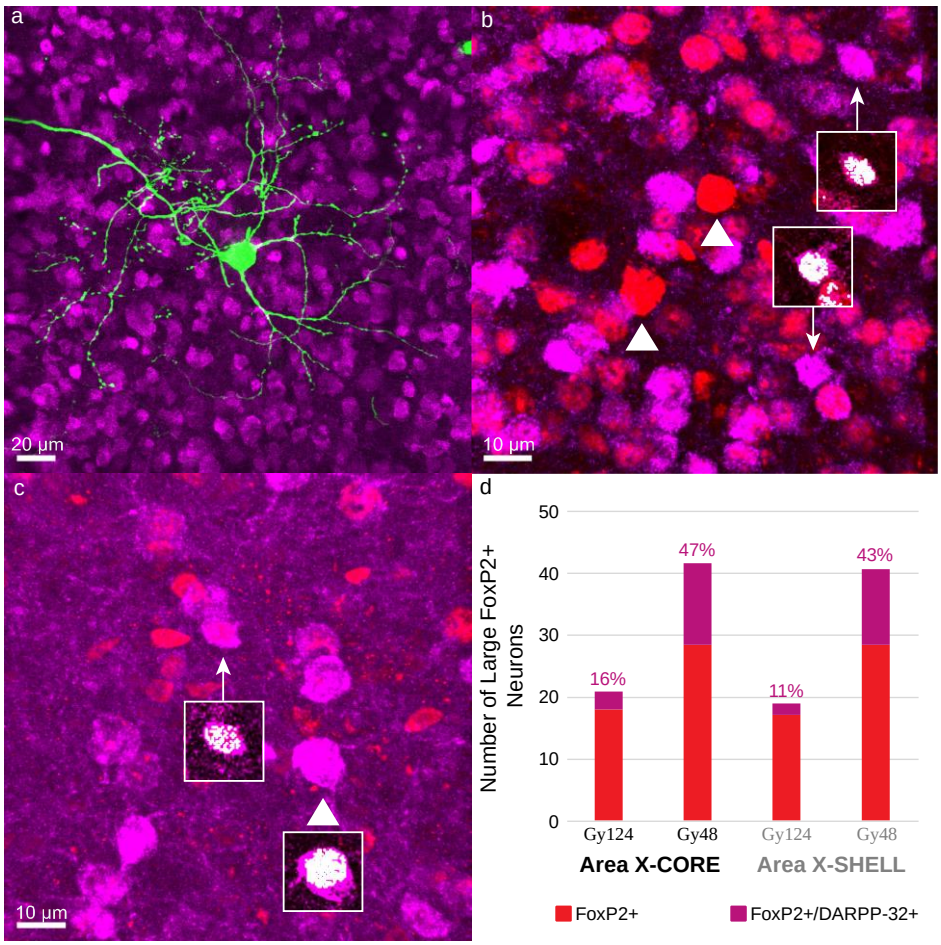

Figure 6. All DIR and most putative IND neurons did not express the striatal marker DARPP-32 in juvenile songbirds. (a) Alexa 488-labeled DIR DLM-projecting neurons (one shown from Area X-CORE) did not colocalize with magenta cytoplasmic DARPP-32 label. (b) Most large (≥8 µm) putative IND FoxP2+ nuclei across both Area X-CORE and SHELL did not express DARPP-32; two examples from Area-X CORE are indicated by white arrowheads. A majority of small (<8 µm) FoxP2+ nuclei expressed DARPP-32 (two examples indicated by white arrows). Insets depict the colocalization of both proteins in white. (c) Some large (≥8 µm) FoxP2+ nuclei expressed DARPP-32 in both CORE and SHELL regions of Area X; white arrowhead indicates a large FoxP2+/DARPP-32+ neuron from Area-X SHELL. An adjacent small (<8 µm; white arrow) FoxP2+ nucleus also expressed DARPP-32. Colocalization insets show that the FoxP2+ nuclei of the putative IND and medium spiny neuron take up a large percentage of the DARPP-32+ cytoplasm. (d) Bar graph detailing the proportion of large

FoxP2+ neurons that show DARPP-32 expression in Area X-CORE (17/49 neurons) and Area X-SHELL (15/48 neurons) from two juvenile songbirds.

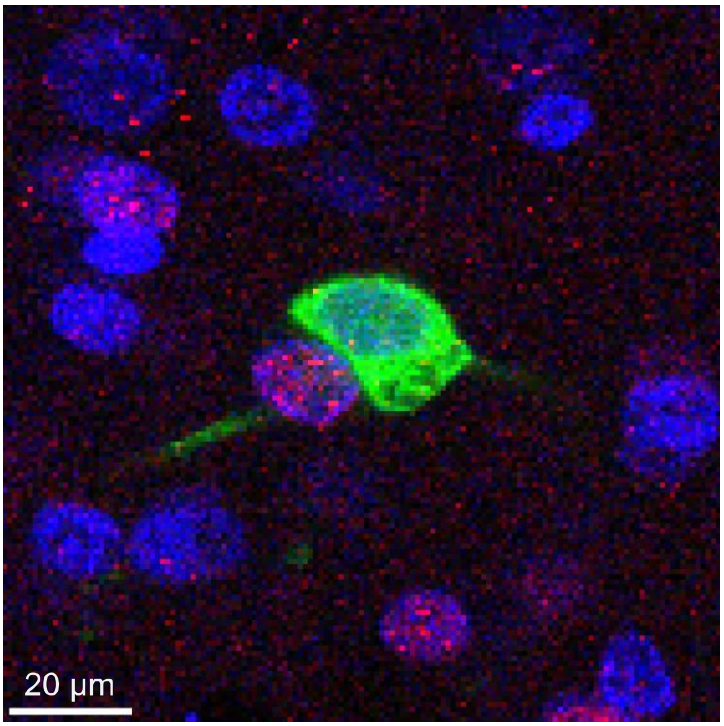

Figure 7. DLM-projecting DIR pallidal cell and adjacent FoxP2+ neuron have similar DAPI+ nuclear sizes. The nucleus of a green Alexa 488+ retrogradely-labeled cell is defined by blue DAPI nuclear stain in Area X-CORE of an adult bird. DAPI+ nucleus of DIR neuron encompasses a smaller percentage of the soma in comparison to putative IND large FoxP2+/DARPP-32+ cells (see Fig. 6c); this pattern was also present in Area X-SHELL (not shown). The adjacent red FoxP2+ nucleus may represent an interneuron or a medium spiny neuron.

Label	Type of stain	Excitation/emission (nm)	Color in figures
DAPI	Nuclear	410/497	Blue
DLM-projecting Alexa Fluor 488	Cytoplasmic	500/580	Green
FoxP2 Alexa Fluor 594	Nuclear	589/651	Red
DARPP-32 Alexa Fluor 647	Cytoplasmic	653/755	Magenta

Table 1. Fluorescent label, type of cellular stain, confocal microscopy excitation/emission wavelengths, and color used in figures for each label in the experiment.

Bird ID	Age (days post-hatch)	# of DIR neurons in Area X-CORE	# of DIR neurons in Area X-SHELL	# of DIR neurons on border of Area X-CORE and Area X-SHELL
Db51	167	98	30	10
Db69	182	39	31	26
R27	104	58	55	20
R54	91	47	52	3
	ADULT TOTAL = 469	**242**	**168**	**59**
Gy48	44	9	8	4
Gy124	46	27	15	18
O63	45	2	3	1
	JUVENILE TOTAL = 87	**38**	**26**	**23**

Table 2. Age and number of DLM-projecting DIR neurons in Area X-CORE and Area X-SHELL. If the DAPI staining was poor on a given tissue section and could not be used to define the precise borders of Area X-CORE, the DLM-projecting direct neurons were placed in the "Border" column.

	Area X-CORE		Area X-SHELL	
	Large FoxP2+	Small FoxP2+	Large FoxP2+	Small FoxP2+
Adult	8.52 ± 0.48 µm n = 102 2.58%	5.38 ± 0.97 µm n = 3851 97.42%	8.34 ± 0.38 µm n = 40 2.61%	5.48 ± 0.99 µm n = 1495 97.39%
Juvenile	8.56 ± 0.49 µm n = 49 2.70%	5.88 ± 1.03 µm n = 1765 97.30%	8.53 ± 0.47 µm n = 48 5.75%	5.73 ± 1.14 µm n = 787 94.25%

Table 3. Mean diameter, cell count, and relative percentage for large (≥8 µm) and small (<8 µm) FoxP2+ nuclei in Area X-CORE and Area X-SHELL of adults and juveniles.